
Kara: Sliding-Window KV Cache Compression for Efficient Serving of Reasoning LLMs under Memory Constraints

Han Shen* kingsutherszs48@gmail.com **Yuyang Wu*** Carnegie Mellon University yuyangwu@cs.cmu.edu **Junpu Yu** Carnegie Mellon University

Olexandr Isayev[†]
Carnegie Mellon University

Abstract

Reasoning language models often generate long chain-of-thought (CoT), which accumulates a massive KV cache during the decoding phase and incurs high decoding latency and limited output throughput. To address these issues, KV cache compression has emerged as a promising technique for reducing memory footprint by selectively removing unimportant KV pairs while preserving useful ones for subsequent decoding. Nevertheless, we identify two key limitations in existing KV cache compression methods: 1) Their threshold-triggered compression policy may reduce output throughput under memory-constrained concurrent serving, and may fully eliminate KV pairs from certain blocks of the sequence, potentially worsening information loss. 2) They typically retain either isolated KV pairs or fixed-size chunks with rigid boundaries, failing to preserve flexible-sized chunks at arbitrary token positions. To overcome these limitations, we propose Kara, a sliding-window KV cache compression method that performs decoding-time compression by operating only on the recently generated context. Kara leverages bidirectional attention to score and select informative KV pairs in the window. To enable flexible preservation of important semantic information, we design a Token2Chunk module to expand a subset of selected KV pairs into chunks. Furthermore, we adapt Kara to PagedAttention and develop KvLLM, an inference framework built upon vLLM, which reduces KV cache memory usage and improves output throughput in memory-constrained environments. Kara preserves nearly 100% of the full-KV accuracy while retaining only 20% of the KV cache, and KvLLM improves throughput by 12.75% on average over vanilla vLLM under memory-constrained concurrent serving.

1 Introduction

Chain-of-thought reasoning [1, 2, 3, 4] has endowed LLMs with powerful capabilities for solving complex tasks. However, reasoning models often generate long traces, which lead to a substantial growth of KV cache during decoding and impose significant memory overhead [5, 6]. For example, caching 128K tokens in Qwen3-14B with FP16 precision requires approximately 20 GB of memory [3]. This overhead becomes especially pronounced in memory-constrained concurrent serving settings, where the rapidly growing KV cache increases decoding latency and causes input requests to wait for available memory resources, thereby reducing overall output throughput.

*Han Shen and Yuyang Wu are co-first authors and contribute equally to this paper.

[†]Corresponding Author

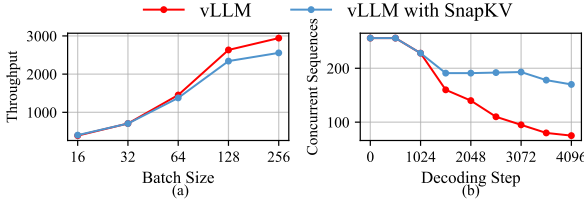


Figure 1: (a) Average output throughput under different batch sizes (*i.e.*, the predefined maximum number of decoding sequences). (b) The actual number of decoding sequences varies with decoding steps. The decoding step denotes the number of global decoding iterations. The predefined maximum number of concurrently decoding sequences is set to 256. SnapKV constrains the KV cache size, freeing memory to decode more sequences concurrently.

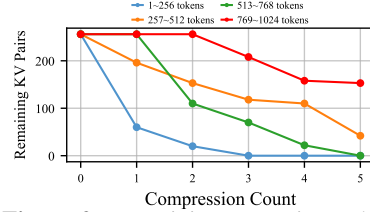


Figure 2: Remaining KV pairs under different compression counts. We track the remaining KV pairs of tokens from different regions for a certain attention head across repeated compression steps. We observe that the semantic information of certain regions is completely eliminated as compression proceeds.

To address these issues, KV cache compression [7, 8, 9], an inference-time approach, has garnered increasing attention. By selectively retaining important KV pairs, KV cache compression can reduce memory usage while keeping performance degradation within an acceptable range (*e.g.*, within a 1% performance drop) [10]. Existing works [9, 10] have shown strong performance on multiple tasks while retaining only a small fraction of the KV cache (*e.g.*, 30%). Early compression methods [11, 12] relied on heuristic techniques such as attention sinks to preserve KV pairs at fixed positions, ignoring the varying importance of different tokens and resulting in suboptimal performance. More recently, research has shifted toward score-based KV cache compression [7, 9, 13, 14], which assigns importance scores to multi-head KV pairs to determine cache retention. These methods typically maintain a query cache of recent query states and use them to score historical KV pairs via attention with their key states. The score-based compression methods often achieve state-of-the-art performance, as they leverage the internal information of LLMs to identify critical KV pairs [15].

Despite their success, we identify two key limitations in existing decoding-time KV cache compression methods:

- **These methods mainly rely on a threshold-triggered compression policy, which can degrade both reasoning performance and inference efficiency.** Under the threshold-triggered compression policy, the KV cache is compressed back to a smaller target length once it reaches a predefined threshold, after which this grow-and-compress pattern repeats. While effective in low-frequency or personal deployment settings, this policy can cause a concurrency-throughput inversion effect under memory-constrained concurrent serving. Specifically, when the number of concurrently decoding sequences approaches the gap between the threshold and the compressed cache length, compression may be triggered frequently, and the associated computational overhead can outweigh the throughput benefits even as the number of concurrently decoding sequences increases. In addition, since compression is applied over the entire KV cache, previously compressed regions of the sequence may be compressed again, which can further worsen information loss. To empirically validate these challenges, we conduct a simple experiment using the vLLM³ framework [16] with a representative decoding-time compression method (SnapKV[9]) on the MATH-500 dataset [17] with distilled Llama-8B models [18]. As shown in Figure 1, vLLM with SnapKV achieves lower output throughput than vanilla vLLM as the batch size increases (*e.g.*, an average 11.15% drop at batch size 128), even though it consistently maintains a higher actual number of concurrently decoding sequences than vanilla vLLM. In Figure 2, the corresponding KV pairs of the earlier tokens are almost completely removed as compression is applied repeatedly. Detailed experimental settings are provided in Appendix B.1.
- **These methods retain either isolated KV pairs or fixed-size chunks with rigid boundaries, failing to preserve important flexible-sized chunks at arbitrary token positions.** Mainstream KV cache compression methods select isolated KV pairs for retention, which can lead to significant loss of semantic information [19]. To address this issue, several methods [19, 20] further propose retaining contiguous KV pairs to form chunks. For example, ChunkKV [19] partitions the historical KV cache into chunks of the same length with fixed boundaries. However, such retention paradigms

³We use nano-vLLM for our experiments. It retains the core mechanisms of vLLM, including PagedAttention, continuous batching, tensor parallelism, and recomputation, and is convenient for further development

are often rigid and fail to capture flexible-sized KV information distributed at arbitrary positions across the sequence.

To overcome these limitations, we propose Kara, a sliding-window KV cache compression method that performs decoding-time compression only on the recently generated context. Through empirical analysis, we find that the accumulated bidirectional attention received by each KV pair serves as an effective indicator of its importance and informativeness. Building on this observation, Kara uses the accumulated bidirectional attention score as the importance measure to identify discrete candidate KV pairs within the window. To preserve flexible-sized contiguous KV pairs at arbitrary positions, we introduce a simple yet effective Token2Chunk module. Given the candidate discrete KV pairs, Token2Chunk treats every two consecutive candidate KV pairs as the endpoints of a chunk, and filters chunks according to their length and the importance scores of the endpoint KV pairs. Finally, we preserve the candidate discrete KV pairs as well as all KV pairs inside the selected chunks. In summary, Kara produces a compressed KV cache that combines both isolated KV pairs and chunk-level KV pairs within the sliding window. Furthermore, we adapt Kara to PagedAttention [16] and develop KvLLM⁴, a vLLM-based [16] inference framework equipped with a periodic compression policy. To avoid frequent compression triggering during decoding, the periodic compression policy compresses the trailing blocks of selected sequences every fixed number of decoding steps, which controls when compression is triggered. Kara preserves nearly 100% of the full-KV accuracy while retaining only 20% of the KV cache, and KvLLM improves output throughput by 12.75% on average over vanilla vLLM under memory-constrained concurrent serving.

In summary, our main contributions are as follows:

- We propose Kara, a KV cache compression method that uses sliding-window bidirectional attention to identify candidate discrete KV pairs and employs a Token2Chunk module to generate chunks with contiguous KV pairs.
- We adapt the proposed method to PagedAttention and design the KvLLM inference framework with a periodic compression policy, which can effectively improve output throughput and concurrency in memory-constrained environments compared with existing compression methods.
- For Kara, we conduct reasoning and NIAH evaluations, showing superior accuracy under the same budget. For KvLLM, we measure output throughput and latency, demonstrating improved efficiency over vLLM with the baseline compression method in memory-constrained settings.

2 Related Work

2.1 KV Cache Compression

Early compression methods, such as StreamingLLM [11], preserve KV pairs at fixed prefix positions, ignoring the varying importance of different tokens. Mainstream KV cache compression methods [7, 9, 21, 22, 23] leverage LLM-internal query signals to score historical KV pairs and typically achieve state-of-the-art compression performance. Nevertheless, most methods rely on a threshold-triggered policy for decoding-time compression, which may degrade output throughput under memory-constrained concurrent serving. Some works [13, 24] mitigate the issues induced by this policy by adopting delayed compression. For example, DMS [13] scores KV pairs within a recent sliding window and executes eviction after tokens leave the window. TRIM-KV [24] further introduces a time-decay mechanism on KV importance to avoid immediate eviction after leaving the window. However, these methods may still require frequent eviction operations under concurrency and may eliminate all KV pairs from contiguous spans. Although a few methods [19, 20] propose retaining fixed-length chunks with rigid boundaries, they ignore flexible-sized chunks at arbitrary positions. Different from the above works, we score KV pairs using sliding-window bidirectional attention and introduce Token2Chunk to expand discrete KV pairs into flexible-sized chunks. Note that the sliding window in some works [25, 19] is mainly used to protect recent tokens from compression, whereas in our method it specifies the tokens to be compressed. Furthermore, we adopt a periodic compression policy to compress the trailing window of selected sequences every fixed number of decoding steps, controlling when compression is triggered.

⁴KvLLM is built upon the nano-vLLM framework.

2.2 Sparse Attention

Sparse attention [26, 27, 28, 29] aims to reduce the quadratic attention cost by selectively computing only a subset of attention interactions while omitting the others. Previous works [30] train models to produce a dynamic attention mask before each attention operation, where the mask indicates the currently useful KV information for attention computation and skips the rest. However, these sparse attention methods typically do not reduce the KV cache memory footprint, and they need to be applied at every decoding step [30]. With the development of LLMs, recent works [31, 32] have moved toward hybrid attention that incorporates sparse attention with compressed attention to address the memory-bound nature of decoding. For example, DeepSeek-V4’s heavily compressed attention [31] merges the KV pairs of contiguous tokens within a long span into a single entry, which effectively reduces the KV cache memory footprint. Our sliding-window compression shares a similar intuition with DeepSeek-V4’s compressed attention: both aim to perform block-level compression to preserve local contextual information while reducing KV cache memory, and DeepSeek-V4 performs KV merging whereas we perform KV eviction. The key difference lies in the training requirement, in which compressed attention typically requires LLM-coupled pretraining, while our method is training-free and can be applied as a plug-in to a broad range of LLMs.

3 Preliminary

Notation. We consider an autoregressive Transformer-based LLM [33, 34] that generates a token sequence denoted by $\mathbf{X} = (x_1, x_2, \dots, x_S)$, where S is the sequence length. The model consists of L Transformer layers, each with H attention heads and head dimension d . For the h -th attention head, we denote the projected query, key, and value states as $\mathbf{Q}^{l,h}, \mathbf{K}^{l,h}, \mathbf{V}^{l,h} \in \mathbb{R}^{S \times d}$, respectively. In layer l and head h , the scaled dot-product attention probabilities are defined as:

$$\mathbf{P}^{l,h} = \text{softmax}\left(\frac{\mathbf{Q}^{l,h}(\mathbf{K}^{l,h})^\top}{\sqrt{d}} + \mathbf{M}\right), \quad (1)$$

where $\mathbf{P}_{i,j}^{l,h}$ denotes the attention probability from the i -th query token to the j -th key token, the causal attention mask \mathbf{M} is an upper triangular matrix with nonzero values of $-\infty$. For simplicity, we use \mathbf{Q} and \mathbf{K} to denote the query and key states of a specific layer l and head h .

LLM Inference. During autoregressive decoding, the model maintains a key cache \mathcal{K} and a value cache \mathcal{V} to store the key and value states corresponding to prefix tokens. KV caching avoids recomputing attention over the entire prefix from scratch and improves inference efficiency [35].

In practice, the decoding efficiency of LLMs is commonly measured by TPOT (Time Per Output Token), which denotes the average time required to generate one output token during decoding and reflects the decoding latency. Beyond TPOT, throughput is another important metric that measures the number of output tokens generated per unit time, and is commonly used to reflect the concurrency. In general, more concurrently decoding sequences enable higher throughput. In long-context scenarios, the inference overhead may be dominated by memory access to the KV cache, leaving the decoding phase memory-bound. We present the formulas of TPOT and throughput in Appendix C.1.

To improve the serving efficiency of LLM inference, frameworks [16, 36] such as vLLM have been widely developed, and they aim to maximize memory utilization and sustain efficient decoding under high-concurrency and long-context generation. The core idea of vLLM is PagedAttention, which views the KV cache as a group of fixed-size blocks. Each block stores a contiguous segment of KV pairs (e.g., 256 tokens), and memory allocation and release are managed at the block level during inference. However, in memory-constrained settings, the available memory can be rapidly consumed as decoding proceeds, which may force the inference framework to reduce the number of running requests and thereby limit overall output throughput (shown in Figure 1 (b)).

KV Cache Compression. Most compression methods [7, 9, 10, 37] estimate an importance score $\mathbf{A}_i^{l,h}$ for the i -th KV cache entry in attention head h and layer l , and then select the most important KV pairs under a cache budget when the cache length reaches a predefined threshold. A representative score-based compression paradigm can be formulated as:

$$\mathcal{I}^{l,h} = \text{TopK}(\{\mathbf{A}_i^{l,h}\}_{i=1}^{C_t}, N) \quad (2)$$

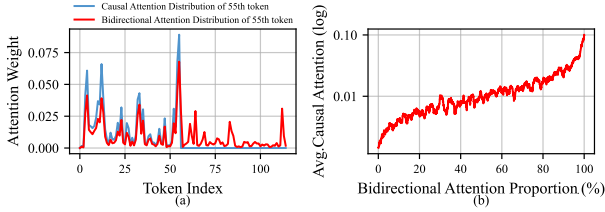


Figure 3: (a) Distribution comparison between causal attention and bidirectional attention of a specific token. (b) Average causal attention weight versus bidirectional attention percentile. We first compute the bidirectional attention weights for all token pairs (x_i, x_j) with $j > i$, using x_i as the query and x_j as the key. We then sort these weights in ascending order and group the pairs by percentiles. Finally, for each percentile group, we compute the causal attention weight for the same pairs in the reverse direction (x_j as the query and x_i as the key), average the causal attention weights within the group, and plot the resulting averages against the bidirectional-attention percentiles.

$$(\mathcal{K}^{l,h}, \mathcal{V}^{l,h}) \leftarrow (\mathcal{K}^{l,h}, \mathcal{V}^{l,h})[\mathcal{I}^{l,h}], \quad \text{when } C_t \geq C_{\max}, \quad (3)$$

where $\mathcal{I}^{l,h}$ is the index of selected KV pairs of head h and layer l , N is the predefined KV budget, C_t denotes the number of KV pairs currently stored in the cache (*i.e.*, the cache length) at decoding step t , C_{\max} denotes the predefined threshold. Once compressed, the cache length is constrained within the interval $[N, C_{\max}]$ as it grows from N back to C_{\max} before the next compression. Existing methods often set the gap between the budget and the threshold to 128 or 256 to obtain optimal performance [7, 15]. In the following, we omit the notation l and h as all operations performed in the layer and attention head are the same in our method. Although the compression paradigm in Equation (2) and (3) is widely adopted, it suffers from two key limitations:

- **Threshold-triggered compression may degrade both reasoning performance and inference efficiency.** Since the paradigm operates compression over the entire KV cache, it may fully remove all KV pairs within a long contiguous span of context (*e.g.*, $x_1 \sim x_{256}$ in Figure 2), potentially exacerbating information loss. Furthermore, when the number of concurrently decoding sequences increases toward the gap between C_{\max} and N (*i.e.*, $C_{\max} - N$), compression can be triggered frequently across concurrently decoding sequences, making the overall compression overhead more pronounced and potentially reducing throughput (shown in Figure 1).
- **Retention granularity is often either isolated KV pairs or rigid fixed-size chunks.** Mainstream score-based methods select isolated KV pairs for retention, which can lead to the loss of semantic information. Although some methods retain contiguous KV pairs to form chunks, such chunks are often extracted with rigid boundaries (*e.g.*, from x_1 to x_{10}), which may fail to capture flexible-sized cache information distributed at arbitrary positions across the sequence.

Given the flaws of existing methods, we argue for using sliding-window bidirectional-attention scores to guide KV-pair retention within the window, together with a retention strategy that incorporates both token-level and chunk-level KV pairs. We further adapt our method to PagedAttention and develop the KvLLM framework with a periodic compression policy, which aims to improve throughput under high concurrency by controlling when compression is triggered.

4 Method

4.1 Sliding-Window Bidirectional Attention for KV Importance Estimation

During decoding, we maintain a sliding window that dynamically covers recently generated tokens, and we apply KV cache compression only to KV pairs within the window. Once compression is performed, the window slides forward to cover newly generated tokens that are uncompressed, and the same procedure is applied repeatedly. Inspired by [7] and [9], we additionally reserve a buffer at the end of the window to protect the latest generated tokens from being compressed, which helps preserve reasoning quality.

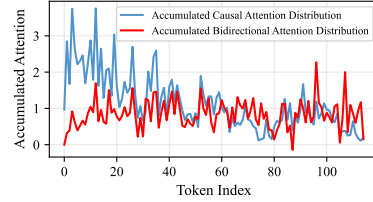


Figure 4: Comparison between accumulated causal attention and bidirectional attention distributions. We compute causal attention and bidirectional attention probability matrices in a given sequence and accumulate the attention received by each token, respectively.

To obtain important discrete KV pairs, we first extract the query states of all tokens inside the window and compute bidirectional attention to the key states of tokens inside the window except those in the buffer. We then accumulate the attention weights received by each KV pair to estimate its importance score. Finally, we select the TopK important KV pairs inside the window as retention candidates. In summary, the sliding-window bidirectional attention scoring can be formulated as:

$$\mathbf{A} = \text{colsum}(\text{softmax}(\frac{\mathbf{Q}_{\mathcal{W}}\mathbf{K}_{\mathcal{W}\setminus\mathcal{U}}^{\top}}{\sqrt{d}})), \quad (4)$$

$$\mathcal{I} = \text{TopK}(\{\mathbf{A}_j\}_{j \in \mathcal{W}\setminus\mathcal{U}}, \lceil r(|\mathcal{W}| - |\mathcal{U}|) - \alpha \rceil). \quad (5)$$

where \mathcal{W} denotes the set of token indices in the current sliding window (*i.e.*, $\mathcal{W} = \{1, \dots, |\mathcal{W}|\}$), and $\mathbf{Q}_{\mathcal{W}} \in \mathbb{R}^{|\mathcal{W}| \times d}$ is the query matrix of the tokens in the sliding window \mathcal{W} . $\mathcal{U} \subset \mathcal{W}$ denotes the buffer at the end of the window (*i.e.*, $\mathcal{U} = \{|\mathcal{W}| - |\mathcal{U}| + 1, \dots, |\mathcal{W}|\}$). $\mathcal{W} \setminus \mathcal{U}$ is the compressible region in the window (*i.e.*, $\mathcal{W} \setminus \mathcal{U} = \{1, \dots, |\mathcal{W}| - |\mathcal{U}|\}$). $\mathbf{K}_{\mathcal{W}\setminus\mathcal{U}} \in \mathbb{R}^{|\mathcal{W}\setminus\mathcal{U}| \times d}$ is the key matrix of the tokens in the compressible region $\mathcal{W} \setminus \mathcal{U}$. The $\text{softmax}(\cdot)$ is applied over the key dimension and $\text{colsum}(\cdot)$ denotes summing over all queries. $\mathbf{A} \in \mathbb{R}^{|\mathcal{W}\setminus\mathcal{U}|}$ denotes the estimated importance scores of the KV pairs in the compressible region $\mathcal{W} \setminus \mathcal{U}$. $r \in (0, 1]$ is the overall retention ratio of the compressible region, α is the predefined chunk budget controlling the number of additional KV pairs introduced by Token2Chunk, and \mathcal{I} denotes the index set of candidate discrete KV pairs to be retained within the current window.

Since tokens in \mathcal{U} are excluded from compression in the current window, Equation (4) computes bidirectional attention scores using queries from all tokens in \mathcal{W} , with scoring restricted to the key states in the compressible region $\mathcal{W} \setminus \mathcal{U}$. Equation (5) retains candidate KV pairs in the compressible region $\mathcal{W} \setminus \mathcal{U}$. After compression, the window moves forward by $|\mathcal{W}| - |\mathcal{U}|$ steps once there are $|\mathcal{W}| - |\mathcal{U}|$ newly generated uncompressed tokens beyond the current window. Implementation details of sliding-window bidirectional attention scoring are presented in Appendix C.2.

Empirical Analysis. We conduct simple experiments to illustrate bidirectional attention in importance estimation. Given a sequence, we first compute both the causal attention and bidirectional attention probability matrices, and visualize the cumulative attention received by each token’s key state from all query tokens. As shown in Figure 4, most accumulated causal attention scores concentrate in the prefix region of the window, as earlier positions are accessible to more queries than later ones. Then, we visualize the specific token’s bidirectional attention probability distribution over all tokens in the sequence, as well as its causal attention distribution over its preceding tokens. As shown in Figure 3(a), we observe that the bidirectional attention distribution of the token at the preceding positions largely matches its causal attention distribution. Finally, we examine the correlation between the bidirectional attention probability from the earlier token x_i to the later token x_j ($j > i$) and the causal attention probability from later token x_j to the earlier token x_i . In Figure 3 (b), we observe that when the earlier token x_i assigns a higher bidirectional attention weight to future token x_j , token x_j also tends to assign a higher causal attention weight to the earlier token x_i .

The above analyses suggest that bidirectional attention can identify important preceding information and highlight future tokens that assign high attention weight to the preceding tokens. These future tokens often contain rich contextual information. Building on this observation, we use bidirectional attention to identify KV pairs that are both important and informative for the current window (more results are presented in Appendix D.1).

4.2 Token2Chunk Module

Building on the discrete KV indices \mathcal{I} obtained from sliding-window bidirectional attention, we introduce a lightweight Token2Chunk module to preserve flexible-sized contiguous KV pairs at arbitrary positions within the window. Specifically, Token2Chunk takes as input discrete retained indices \mathcal{I} and the corresponding importance scores $\mathbf{A} \in \mathbb{R}^{|\mathcal{W}\setminus\mathcal{U}|}$. We first define the chunk budget that controls the maximum number of additional KV pairs that can be introduced by this module, together with a maximum chunk length. We then sort the indices in \mathcal{I} in ascending order and divide the compressible region into chunks by treating every two KV pairs that are consecutive in the sorted index set as the endpoints of a candidate chunk (not adjacent in the original sequence). Each candidate chunk indicates a contiguous span, whose interior positions correspond to KV pairs that

can be additionally retained as a chunk. Next, we filter candidate chunks by the maximum chunk length, and score each remaining chunk using both its length and the importance scores of the two endpoint KV pairs. Finally, we preserve all KV pairs inside the selected chunks, and union them with \mathcal{I} to obtain the final retained indices. For the k -th chunk ($1 \leq k \leq |\mathcal{I}| - 1$), Token2Chunk can be formulated as:

$$\mathbf{R}_k = (\mathbf{A}_{\mathcal{I}[k]} + \mathbf{A}_{\mathcal{I}[k+1]}) \times (\mathcal{I}[k+1] - \mathcal{I}[k] - 1), \quad (6)$$

$$\mathcal{P} = \text{TopK}(\{\mathbf{R}_k\}_{k=1}^{|\mathcal{I}|-1}, \left\lfloor \frac{\alpha}{\gamma - 2} \right\rfloor), \quad \text{s.t. } \mathcal{I}[k+1] - \mathcal{I}[k] < \gamma \quad (7)$$

$$\hat{\mathcal{I}} = \mathcal{I} \cup \bigcup_{k \in \mathcal{P}} \{j \mid \mathcal{I}[k] < j < \mathcal{I}[k+1]\}. \quad (8)$$

where \mathbf{R}_k is the k -th chunk’s retention score, \mathcal{I} is the discrete retained indices obtained from sliding-window bidirectional attention (sorted in ascending order), and $\mathcal{I}[k]$ denotes the k -th smallest element in \mathcal{I} . $\mathbf{A}_{\mathcal{I}[k]}$ is the importance score of the KV pair at index $\mathcal{I}[k]$. γ is the predefined maximum chunk length (including two endpoints) and $\gamma \geq 3$, and α is the predefined chunk budget controlling the number of additional KV pairs introduced by Token2Chunk. \mathcal{P} denotes selected chunk indices returned by $\text{TopK}(\cdot)$, and $\hat{\mathcal{I}}$ denotes the final retained KV pair indices after adding all KV pairs inside the selected chunks. We then use $\hat{\mathcal{I}}$ to compress the KV cache of the current sliding window:

$$(\mathcal{K}_{\mathcal{W} \setminus \mathcal{U}}, \mathcal{V}_{\mathcal{W} \setminus \mathcal{U}}) \leftarrow (\mathcal{K}_{\mathcal{W} \setminus \mathcal{U}}, \mathcal{V}_{\mathcal{W} \setminus \mathcal{U}})[\hat{\mathcal{I}}], \quad (9)$$

where $(\mathcal{K}_{\mathcal{W} \setminus \mathcal{U}}, \mathcal{V}_{\mathcal{W} \setminus \mathcal{U}})$ denotes the KV cache of the compressible region within the current sliding window.

In Equation (6), the first term measures chunk importance using the importance scores of two consecutive indices in \mathcal{I} , which serve as the start ($\mathcal{I}[k]$) and end ($\mathcal{I}[k+1]$) positions of the chunk. The second term captures the chunk length, and a longer chunk preserves more contextual information. Equation (7) selects the chunks with TopK scores under the maximum-length constraint. Implementation details of Token2Chunk are presented in Appendix C.3. We visualize the retained positions before and after applying Token2Chunk in Appendix D.2.

4.3 KvLLM: Periodic Compression with PagedAttention

We adapt Kara to PagedAttention and develop KvLLM, an inference framework that supports applying KV cache compression to improve decoding efficiency in memory-constrained environments. To mitigate the concurrency-throughput inversion effect observed in Figure 1, KvLLM adopts a periodic compression policy that is aligned with Kara’s sliding-window design. The pseudo-code and implementation details of the periodic policy are shown in Appendix C.4. Generally, KvLLM maintains a global decoding-step counter from the beginning of inference and applies a periodic compression schedule. Specifically, we first set the number of decoding steps between two consecutive compression events. Then, at each scheduled compression, KvLLM selects a subset of running sequences whose trailing PagedAttention blocks are still uncompressed. For each selected sequence, KvLLM treats its trailing blocks as a compression window and applies Kara to compress the KV cache within this window. Finally, KvLLM performs post-processing, including memory compaction and block release. By controlling when compression is triggered, periodic compression avoids frequent triggering across concurrent requests. Under memory-constrained concurrent serving, KvLLM reduces the KV cache footprint and frees memory to decode more sequences. The overall complexity of Kara is presented in Appendix D.6.

5 Experiments

Benchmarks. We evaluate on three mathematical reasoning benchmarks: MATH-500[17], AIME 2024[38], and AMC 2023. We use greedy decoding and report accuracy of zero-shot pass@1, computed as the fraction of problems answered correctly. We set the maximum generation length to 16,384 tokens for MATH-500 and AMC 2023, and 32,768 tokens for AIME 2024. We also include a long-context evaluation on the Needle-in-a-Haystack (NIAH) benchmark.

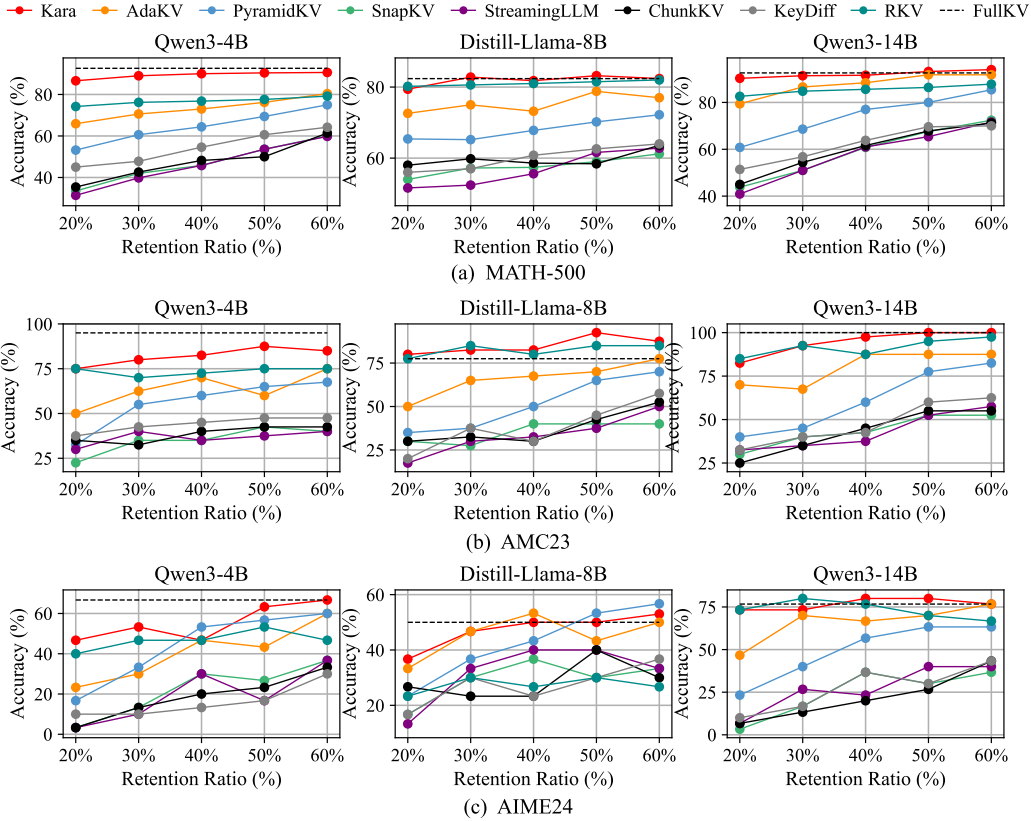


Figure 5: Performance of different KV cache compression methods across varying retention levels. The dash line represents the accuracy of the vanilla LLM model without compression. Note that AdaKV and PyramidKV allocate adaptive memory budgets across layers and heads.

Baselines. We compare Kara against 7 representative decoding-time KV cache compression baselines, including RKV[7], KeyDiff[25], SnapKV [9], StreamingLLM [11], PyramidKV [39], AdaKV [8], and a chunk-based method ChunkKV [19]⁵. For each baseline, we use its best-performing configuration as recommended by the original paper.

Configurations. We conduct experiments on DeepSeek-R1-Distill-Llama-8B (R1-Llama-8B) [1], Qwen3-14B, and Qwen3-4B [3], using BF16 precision. We evaluate the retention ratio $r \in \{20, 30, 40, 50, 60\}\%$, and use the same retention ratio for all layers and attention heads in Kara. Since Kara does not strictly enforce a fixed compressed cache length, different sequences may result in various cache sizes. We ensure a fair comparison by first running Kara to obtain the compressed KV cache length for each sequence and setting the per-sequence KV budget of each baseline to match Kara under the corresponding setting. Note that we evaluate Kara’s reasoning pass@1 without the periodic compression policy for a fair accuracy comparison, since this policy is primarily designed to improve throughput in practical application, and we only activate it in throughput experiments. More hyperparameter settings are presented in Appendix B.3.

5.1 Main Results

Reasoning Performance. Figure 5 reports the reasoning performance of Kara compared with KV cache compression methods under various retention ratios. We observe that: 1) Kara preserves accuracy with no or only minor degradation relative to the vanilla LLM without compression. For example, on MATH-500 with Qwen3-14B, Kara maintains nearly unchanged accuracy at a 30% retention ratio. 2) Kara generally outperforms other compression methods across retention ratios. 3)

⁵Note that ChunkKV was originally designed for token removal during prefill, and we adapt it to decoding-time compression by treating contiguous KV pairs in the cache as a chunk.

Table 1: Ablation study of Kara with Qwen3-4B at a 40% KV retention ratio.

Datasets	MATH-500	AMC23
w/o Bi-Attention	85.20	72.50
w/o Token2Chunk	88.20	77.50
Kara	90.00	82.50

Table 2: Overall inference latency and average throughput under the predefined maximum running sequences.

Metric	128		256	
	Latency (s)	Throughput (tokens/s)	Latency (s)	Throughput (tokens/s)
vLLM	884	2,633	678	2,943
vLLM + SnapKV	920	2,341	738	2,556
KvLLM	864	2,912	640	3,392

Kara outperforms AdaKV and PyramidKV in most cases, which allocate different memory budgets across layers and heads. In contrast, we use a unified configuration and retention ratio for all layers and heads, which is architecturally more compatible with tensor parallelism and PagedAttention in inference frameworks. We further discuss these results in Appendix D.3.

NIAH Performance. To evaluate Kara’s ability to preserve context information under KV cache compression, we conduct a Needle-in-a-Haystack (NIAH) experiment. The results are presented in Appendix D.4. We observe that Kara achieves higher retrieval accuracy than the baselines across most depths and context lengths.

5.2 Ablation Studies

Effects of Bidirectional Attention Scoring. To evaluate the effectiveness of the sliding-window bidirectional attention scoring in Equation (4), we remove bidirectional attention and score KV pairs in the compressible region using only the query states from the protected buffer \mathcal{U} (denoted as w/o Bi-Attention). As shown in Table 1, removing bidirectional attention consistently reduces reasoning accuracy. These results indicate that utilizing all query states in the window with bidirectional attention provides a stronger importance signal than buffer-only causal attention scoring, leading to better preservation of important and informative context.

Effects of Token2Chunk. To assess the effectiveness of the Token2Chunk module in Equation (6), we remove Token2Chunk and retain KV pairs using only bidirectional attention scoring, selecting a target number of discrete KV pairs under the same retention ratio (w/o Token2Chunk). As shown in Table 1, removing Token2Chunk leads to lower performance under compression. These results show that preserving flexible-sized chunks at arbitrary positions helps preserve more semantic context.

5.3 KvLLM Throughput and Latency Evaluation.

To evaluate the efficiency benefits of Kara in practical serving, we adapt it to PagedAttention and develop the KvLLM inference framework. We report both average throughput and overall inference latency for KvLLM, vanilla vLLM, and vLLM equipped with SnapKV under the predefined maximum number of concurrently decoding sequences 128 and 256. For a fair comparison, we simulate a memory-constrained environment for all frameworks, and the detailed settings are presented in Appendix B.1. The results are shown in Table 2. We observe that KvLLM with periodic compression improves output throughput and reduces decoding latency across these settings. The improvement can be attributed to the PagedAttention blocks freed by each compression. These freed blocks can then be used to decode other waiting sequences, thereby increasing throughput and reducing latency. In contrast, the threshold-triggered policy of vLLM+SnapKV can trigger compression frequently. In addition, the accumulated overhead of query buffer maintenance and global memory compaction outweighs the throughput gain from compression. Instead, KvLLM controls when compression is triggered and recomputes query states within the window. It compacts cache memory only in the window region. Overall, these results show that KvLLM, which combines periodic compression with

sliding-window compression, effectively improves throughput and reduces latency under memory constraints. Additional discussion and results on more batch sizes, and the actual concurrency across decoding steps are provided in Appendix D.5.

6 Conclusion

We propose Kara, a decoding-time sliding-window KV cache compression method that scores and retains KV pairs in the recent context using bidirectional attention and augments discrete retention with a Token2Chunk module for flexible-sized chunks. We further integrate it into PagedAttention and develop the KvLLM framework with periodic trailing-block compression to reduce KV-cache memory usage and improve throughput. In the future, we plan to combine KV offloading and retrieval to enable lossless KV cache compression.

7 Acknowledgement

We thank Yang Zhou and Beidi Chen group for their helpful discussions, valuable feedback, and support throughout this project.

References

- [1] Daya Guo, Dejian Yang, Haowei Zhang, Junxiao Song, Peiyi Wang, Qihao Zhu, Runxin Xu, Ruoyu Zhang, Shirong Ma, Xiao Bi, et al. Deepseek-r1: Incentivizing reasoning capability in llms via reinforcement learning. *arXiv preprint arXiv:2501.12948*, 2025.
- [2] Jason Wei, Xuezhi Wang, Dale Schuurmans, Maarten Bosma, Fei Xia, Ed Chi, Quoc V Le, Denny Zhou, et al. Chain-of-thought prompting elicits reasoning in large language models. *Advances in neural information processing systems*, 35:24824–24837, 2022.
- [3] An Yang, Anfeng Li, Baosong Yang, Beichen Zhang, Binyuan Hui, Bo Zheng, Bowen Yu, Chang Gao, Chengen Huang, Chenxu Lv, et al. Qwen3 technical report. *arXiv preprint arXiv:2505.09388*, 2025.
- [4] Debangshu Banerjee, Tarun Suresh, Shubham Ugare, Sasa Misailovic, and Gagandeep Singh. CRANE: Reasoning with constrained LLM generation. In *Forty-second International Conference on Machine Learning*, 2025.
- [5] Haoyang Li, Yiming Li, Anxin Tian, Tianhao Tang, Zhanchao Xu, Xuejia Chen, Nicole Hu, Wei Dong, Qing Li, and Lei Chen. A survey on large language model acceleration based on kv cache management. *arXiv preprint arXiv:2412.19442*, 2024.
- [6] Zhihang Yuan, Yuzhang Shang, Yang Zhou, Zhen Dong, Zhe Zhou, Chenhao Xue, Bingzhe Wu, Zhikai Li, Qingyi Gu, Yong Jae Lee, et al. Llm inference unveiled: Survey and roofline model insights. *arXiv preprint arXiv:2402.16363*, 2024.
- [7] Zefan Cai, Wen Xiao, Hanshi Sun, Cheng Luo, Yikai Zhang, Ke Wan, Yucheng Li, Yeyang Zhou, Li-Wen Chang, Jiuxiang Gu, Zhen Dong, Anima Anandkumar, Abedelkadir Asi, and Junjie Hu. R-KV: Redundancy-aware KV cache compression for reasoning models. In *The Thirty-ninth Annual Conference on Neural Information Processing Systems*, 2026.
- [8] Yuan Feng, Junlin Lv, Yukun Cao, Xike Xie, and S Kevin Zhou. Ada-KV: Optimizing KV cache eviction by adaptive budget allocation for efficient LLM inference. In *The Thirty-ninth Annual Conference on Neural Information Processing Systems*, 2026.
- [9] Yuhong Li, Yingbing Huang, Bowen Yang, Bharat Venkitesh, Acyr Locatelli, Hanchen Ye, Tianle Cai, Patrick Lewis, and Deming Chen. SnapKV: LLM knows what you are looking for before generation. In *The Thirty-eighth Annual Conference on Neural Information Processing Systems*, 2024.

- [10] Jiayi Yuan, Hongyi Liu, Shaochen Zhong, Yu-Neng Chuang, Songchen Li, Guanchu Wang, Duy Le, Hongye Jin, Vipin Chaudhary, Zhaozhuo Xu, Zirui Liu, and Xia Hu. KV cache compression, but what must we give in return? a comprehensive benchmark of long context capable approaches. In Yaser Al-Onaizan, Mohit Bansal, and Yun-Nung Chen, editors, *Findings of the Association for Computational Linguistics: EMNLP 2024*, pages 4623–4648, Miami, Florida, USA, November 2024. Association for Computational Linguistics.
- [11] Guangxuan Xiao, Yuandong Tian, Beidi Chen, Song Han, and Mike Lewis. Efficient streaming language models with attention sinks. In *The Twelfth International Conference on Learning Representations*, 2024.
- [12] Qizhe Zhang, Aosong Cheng, Ming Lu, Renrui Zhang, Zhiyong Zhuo, Jiajun Cao, Shaobo Guo, Qi She, and Shanghang Zhang. Beyond text-visual attention: Exploiting visual cues for effective token pruning in vlms. In *Proceedings of the IEEE/CVF International Conference on Computer Vision*, pages 20857–20867, 2025.
- [13] Adrian Łańcucki, Konrad Staniszewski, Piotr Nawrot, and Edoardo Ponti. Inference-time hyper-scaling with KV cache compression. In *The Thirty-ninth Annual Conference on Neural Information Processing Systems*, 2026.
- [14] Jang-Hyun Kim, Jinuk Kim, Sangwoo Kwon, Jae W. Lee, Sangdoo Yun, and Hyun Oh Song. KVzip: Query-agnostic KV cache compression with context reconstruction. In *The Thirty-ninth Annual Conference on Neural Information Processing Systems*, 2026.
- [15] Alessio Devoto, Maximilian Jeblick, and Simon Jégou. Expected attention: Kv cache compression by estimating attention from future queries distribution. *arXiv preprint arXiv:2510.00636*, 2025.
- [16] Woosuk Kwon, Zhuohan Li, Siyuan Zhuang, Ying Sheng, Lianmin Zheng, Cody Hao Yu, Joseph E. Gonzalez, Hao Zhang, and Ion Stoica. Efficient memory management for large language model serving with pagedattention. In *Proceedings of the ACM SIGOPS 29th Symposium on Operating Systems Principles*, 2023.
- [17] Zicheng Lin, Zhibin Gou, Tian Liang, Ruilin Luo, Haowei Liu, and Yujiu Yang. Criticbench: Benchmarking llms for critique-correct reasoning. In *Findings of the Association for Computational Linguistics: ACL 2024*, pages 1552–1587, 2024.
- [18] Aaron Grattafiori, Abhimanyu Dubey, Abhinav Jauhri, Abhinav Pandey, Abhishek Kadian, Ahmad Al-Dahle, Aiesha Letman, Akhil Mathur, Alan Schelten, Alex Vaughan, et al. The llama 3 herd of models. *arXiv preprint arXiv:2407.21783*, 2024.
- [19] Xiang Liu, Zhenheng Tang, Peijie Dong, Zeyu Li, Liuyue, Bo Li, Xuming Hu, and Xiaowen Chu. ChunkKV: Semantic-preserving KV cache compression for efficient long-context LLM inference. In *The Thirty-ninth Annual Conference on Neural Information Processing Systems*, 2026.
- [20] Emily Xiao, Chin-Jou Li, Yilin Zhang, Graham Neubig, and Amanda Bertsch. Efficient many-shot in-context learning with dynamic block-sparse attention. In Wanxiang Che, Joyce Nabende, Ekaterina Shutova, and Mohammad Taher Pilehvar, editors, *Proceedings of the 63rd Annual Meeting of the Association for Computational Linguistics (Volume 1: Long Papers), ACL 2025, Vienna, Austria, July 27 - August 1, 2025*, pages 31946–31958. Association for Computational Linguistics, 2025.
- [21] Akshat Ramachandran, Marina Neseem, Charbel Sakr, Rangharajan Venkatesan, Brucek Khailany, and Tushar Krishna. ThinKV: Thought-adaptive KV cache compression for efficient reasoning models. In *The Fourteenth International Conference on Learning Representations*, 2026.
- [22] Dalton Jones, Junyoung Park, Matthew J Morse, Mingu Lee, Matthew Harper Langston, and Christopher Lott. QuoKA: Query-oriented KV selection for efficient LLM prefill. In *The Fourteenth International Conference on Learning Representations*, 2026.

- [23] Yuzhen Mao, Qitong Wang, Martin Ester, and Ke Li. Icecache: Memory-efficient KV-cache management for long-sequence LLMs. In *The Fourteenth International Conference on Learning Representations*, 2026.
- [24] Ngoc Bui, Shubham Sharma, Simran Lamba, Saumitra Mishra, and Rex Ying. Cache what lasts: Token retention for memory-bounded KV cache in LLMs. In *The Fourteenth International Conference on Learning Representations*, 2026.
- [25] Junyoung Park, Dalton Jones, Matthew J Morse, Raghav Goel, Mingu Lee, and Christopher Lott. Keydiff: Key similarity-based KV cache eviction for long-context LLM inference in resource-constrained environments. In *The Thirty-ninth Annual Conference on Neural Information Processing Systems*, 2026.
- [26] Jintao Zhang, Chendong Xiang, Haofeng Huang, Jia wei, Haocheng Xi, Jun Zhu, and Jianfei Chen. Spargeattention: Accurate and training-free sparse attention accelerating any model inference. In *Forty-second International Conference on Machine Learning*, 2025.
- [27] Enzhe Lu, Zhejun Jiang, Jingyuan Liu, Yulun Du, Tao Jiang, Chao Hong, Shaowei Liu, Weiran He, Enming Yuan, Yuzhi Wang, Zhiqi Huang, Huan Yuan, Suting Xu, Xinran Xu, Guokun Lai, Yanru Chen, Huabin Zheng, Junjie Yan, Jianlin Su, Yuxin Wu, Yutao Zhang, Zhilin Yang, Xinyu Zhou, Mingxing Zhang, and Jiezhong Qiu. MoBA: Mixture of block attention for long-context LLMs. In *The Thirty-ninth Annual Conference on Neural Information Processing Systems*, 2026.
- [28] Chaofan Lin, Jiaming Tang, Shuo Yang, Hanshuo Wang, Tian Tang, Boyu Tian, Ion Stoica, Song Han, and Mingyu Gao. Twilight: Adaptive attention sparsity with hierarchical top-\$p\$ pruning. In *The Thirty-ninth Annual Conference on Neural Information Processing Systems*, 2026.
- [29] Ruyi Xu, Guangxuan Xiao, Haofeng Huang, Junxian Guo, and Song Han. Xattention: Block sparse attention with antidiagonal scoring. In Aarti Singh, Maryam Fazel, Daniel Hsu, Simon Lacoste-Julien, Felix Berkenkamp, Tegan Maharaj, Kiri Wagstaff, and Jerry Zhu, editors, *Forty-second International Conference on Machine Learning, ICML 2025, Vancouver, BC, Canada, July 13-19, 2025*, Proceedings of Machine Learning Research. PMLR / OpenReview.net, 2025.
- [30] Yutao Sun, Zhenyu Li, Yike Zhang, Tengyu Pan, Bowen Dong, Yuyi Guo, and Jianyong Wang. Efficient attention mechanisms for large language models: A survey. *arXiv preprint arXiv:2507.19595*, 2025.
- [31] DeepSeek-AI. Deepseek-v4: Towards highly efficient million-token context intelligence, 2026.
- [32] Chenglong Chu, Guorui Zhou, Guowang Zhang, Han Li, Hao Peng, Hongtao Cheng, Jian Liang, Jiangxia Cao, Kun Gai, Lingzhi Zhou, et al. Kwai summary attention technical report. *arXiv preprint arXiv:2604.24432*, 2026.
- [33] Suzanna Sia, David Mueller, and Kevin Duh. Where does in-context learning \\\ happen in large language models? In *The Thirty-eighth Annual Conference on Neural Information Processing Systems*, 2024.
- [34] Josh Achiam, Steven Adler, Sandhini Agarwal, Lama Ahmad, Ilge Akkaya, Florencia Leoni Aleman, Diogo Almeida, Janko Altenschmidt, Sam Altman, Shyamal Anadkat, et al. Gpt-4 technical report. *arXiv preprint arXiv:2303.08774*, 2023.
- [35] Haoyang LI, Yiming Li, Anxin Tian, Tianhao Tang, Zhanchao Xu, Xuejia Chen, Nicole HU, Wei Dong, Li Qing, and Lei Chen. A survey on large language model acceleration based on KV cache management. *Transactions on Machine Learning Research*, 2025.
- [36] Lianmin Zheng, Liangsheng Yin, Zhiqiang Xie, Chuyue Sun, Jeff Huang, Cody Hao Yu, Shiyi Cao, Christos Kozyrakis, Ion Stoica, Joseph E. Gonzalez, Clark Barrett, and Ying Sheng. Sglang: efficient execution of structured language model programs. NIPS '24, Red Hook, NY, USA, 2024. Curran Associates Inc.

- [37] Ziran Qin, Yuchen Cao, Mingbao Lin, Wen Hu, Shixuan Fan, Ke Cheng, Weiyao Lin, and Jianguo Li. CAKE: Cascading and adaptive KV cache eviction with layer preferences. In *The Thirteenth International Conference on Learning Representations*, 2025.
- [38] Yifan Zhang and Team Math-AI. American invitational mathematics examination (aime) 2024, 2024.
- [39] Zefan Cai, Yichi Zhang, Bofei Gao, Yuliang Liu, Yucheng Li, Tianyu Liu, Keming Lu, Wayne Xiong, Yue Dong, Junjie Hu, et al. Pyramidkv: Dynamic kv cache compression based on pyramidal information funneling. *arXiv preprint arXiv:2406.02069*, 2024.
- [40] Yao Fu, Rameswar Panda, Xinyao Niu, Xiang Yue, Hannaneh Hajishirzi, Yoon Kim, and Hao Peng. Data engineering for scaling language models to 128k context. ICML’24. JMLR.org, 2024.

A Limitations, Future Work and Impact

Limitations. We acknowledge several limitations of Kara and KvLLM. First, permanently evicting KV pairs inevitably causes information loss and may degrade reasoning performance in broader application settings. Second, obtaining query states via recomputation is straightforward to implement in practice but introduces non-trivial overhead. Although the periodic compression policy can reduce the frequency of recomputation and improve the overall trade-off, the overhead remains a key challenge. Third, compared with threshold-triggered policies, Kara and KvLLM do not precisely control the memory footprint, which may be less suitable for settings with strict memory requirements. Finally, our compression is not global, which may leave redundancy in the KV cache that cannot be fully eliminated.

Future Work. In future work, we plan to incorporate KV cache offloading and retrieval into KvLLM. Concretely, we view a sequence’s KV cache as two parts: KV pairs that remain persistently important over a long horizon, and KV pairs that are only important in the short term. For each sequence, we will additionally maintain a dedicated block to store short-term KV pairs, while the remaining blocks store long-term KV pairs together with the most recently generated KV pairs. For compression, we will continue to use periodic compression with two schedules: a long period for updating the long-term blocks and a short period for updating the short-term block. At each compression event, evicted KV pairs will be moved to CPU memory or SSD, and we will use the latest tokens’ query states to retrieve the TopK KV pairs back into HBM for decoding. This offloading-and-retrieval design can mitigate information loss caused by permanent eviction and improve throughput while reducing GPU-memory usage.

To reduce compression overhead, we will also consider training-based approaches to predict importance scores. To make learned scoring effective across broader settings, such training may need to be integrated with sparse-attention modeling, where importance signals can be learned jointly during pretraining. This direction may enable low-overhead KV cache compression that generalizes to more diverse scenarios.

Broader Impacts. Kara’s sliding-window compression mechanism and KvLLM’s periodic compression policy provide a practical path for deploying and integrating KV cache compression into inference frameworks.

B Detailed Experimental Settings

B.1 Detailed Settings for vLLM and KvLLM

For all frameworks, to simulate a memory-constrained environment, we use DeepSeek-R1-Distill-LLaMA-8B and the MATH-500 dataset (average generation length is approximately 3,000 tokens). We set the tensor-parallel size to 4 and the GPU memory utilization to 0.5 (*i.e.*, 16GB). The maximum sequence generation length is set to 8,192 tokens. We set the block size to 256.

For vLLM+SnapKV, we set the compression threshold to 1280 KV pairs (5 blocks) and set the compressed cache length to 1,025 KV pairs (also 5 blocks). The SnapKV query cache length is 32.

For Kara in KvLLM, we set the window length to 3 PagedAttention blocks (768 KV pairs) and the total retained length per window to 257 KV pairs. The extra KV pair is reserved to avoid frequent block allocation. The compression period is set to 128 decoding steps. At each compression, KvLLM selects 30 sequences whose trailing context contains at least 768 uncompressed tokens and applies Kara within the trailing window. The buffer length is also 32.

All experiments are conducted on 8 RTX 5090 GPUs.

B.2 Detailed Experimental Settings for Figure 3 and 4

This section provides detailed settings for the simple experiment shown in Figure 3 and 4. We conduct this analysis using DeepSeek-R1-Distill-Llama-8B. We sample multiple prompts from the MATH-500 dataset and extract the Q/K/V states of the first 120 tokens. We report a representative example. When analyzing attention, we visualize the attention probability distribution averaged over all attention heads for each token.

B.3 Detailed Experimental Settings in Section 5

Experiments for Kara are conducted on a cluster with 8 H200 GPUs and 8 H100 GPUs. For Kara, we sweep the window length $|\mathcal{W}| \in \{256, 384, 512\}$ and set the buffer length $|\mathcal{U}| \in \{32, 64\}$. For Token2Chunk, we use a fixed maximum chunk size γ of 8 and set the additional chunk budget α to 16 or 32.

C Details

C.1 Formula of TPOT and Throughput

In a simplified decoding setting, where the number of concurrently decoding sequences is denoted by B^6 , the KV cache uses BF16 precision, and the FFN intermediate size is four times the hidden size, the TPOT can be approximated as follows:

$$\text{TPOT} \approx \max\left(\frac{2L(12BD^2 + 2BSD)}{\rho}, \frac{4LBSD}{\beta}\right), \quad (10)$$

where ρ denotes the effective GPU compute throughput, $D = Hd$ is the hidden dimension and β denotes the effective HBM bandwidth, and modern GPUs generally have a high compute-to-bandwidth ratio. The first term in Equation (10) corresponds to the computation cost of one decoding forward step, while the second term captures the memory access overhead of KV cache. We omit the memory footprint of model weights since we focus on the KV cache. The output throughput at each decoding step can be formulated as:

$$\text{Throughput} \approx \frac{B}{\text{TPOT}}, \quad (11)$$

From Equation (10) and 11, we can observe that in long-context reasoning scenarios, the inference overhead may be dominated by memory access to the KV cache, leaving the inference memory-bound, and higher B generally enables higher throughput.

C.2 Implementation Details of Sliding-window Bidirectional Attention Scoring

In this section, we present the implementation details of sliding-window bidirectional attention. We can obtain the query states required for KV scoring by recomputing the current sliding window while reusing the existing KV cache. Specifically, at each compression, in addition to Kara’s computation, we run an additional forward pass on the tokens in the current window. In this pass, we compute only the query projections, the causal attention against the cached prefix KV states, and the FFN (feed-forward network), while reusing the existing key and value caches. This recomputation avoids maintaining an explicit query cache during decoding. The sliding-window mechanism can also be applied to compress the prompt KV cache before decoding. Specifically, during the prefill stage, we can partition the prompt into multiple windows of length $|\mathcal{W}|$ and perform window-wise compression

⁶ B varies dynamically during decoding

Algorithm 1 Periodic compression policy of KvLLM

Require: Running queue \mathcal{Q} , empty key/value caches \mathcal{K} , \mathcal{V} , global step counter $g \leftarrow 0$, compression period δ , compression window length $|\mathcal{W}|$, buffer length $|\mathcal{U}|$, retention ratio r , $\text{Kara}(\cdot)$ (returns retained indices for the compressible region in a trailing window)

```
1: while  $\mathcal{Q} \neq \emptyset$  do
2:   Run one decoding step for sequences in  $\mathcal{Q}$ ; update  $\mathcal{K}$ ,  $\mathcal{V}$ 
3:    $g \leftarrow g + 1$ 
4:   if  $g > |\mathcal{W}|$  and  $g \bmod \delta = 0$  then
5:      $\mathcal{Q}' \leftarrow \text{SELECT}(\mathcal{Q})$   $\triangleright$  select sequences whose trailing  $|\mathcal{W}|$  tokens are uncompressed
6:     for all  $e \in \mathcal{Q}'$  do
7:        $\mathcal{K}_{\mathcal{W}} \leftarrow \mathcal{K}[e, -|\mathcal{W}| : ]$ 
8:        $\mathcal{V}_{\mathcal{W}} \leftarrow \mathcal{V}[e, -|\mathcal{W}| : ]$ 
9:        $\hat{\mathcal{I}} \leftarrow \text{Kara}(\mathcal{K}_{\mathcal{W}}, \mathcal{V}_{\mathcal{W}}, r)$ 
10:       $(\mathcal{K}_{\mathcal{W} \setminus \mathcal{U}}, \mathcal{V}_{\mathcal{W} \setminus \mathcal{U}}) \leftarrow (\mathcal{K}_{\mathcal{W} \setminus \mathcal{U}}, \mathcal{V}_{\mathcal{W} \setminus \mathcal{U}})[\hat{\mathcal{I}}]$ 
11:       $\text{MEMORYCOMPACTION}(e)$ 
12:       $\text{UPDATEMETADATA}(e)$ 
13:    end for
14:  end if
15: end while
```

on the KV pairs corresponding to positions inside each window in parallel. After compression, the window moves forward by $|\mathcal{W}| - |\mathcal{U}|$ steps once there are $|\mathcal{W}| - |\mathcal{U}|$ uncompressed tokens beyond the current window during decoding.

C.3 Implementation Details of Token2Chunk

During decoding, Token2Chunk is applied to the compressible region immediately after the bidirectional-attention scoring stage. Token2Chunk is a lightweight module, and its additional complexity is $O(n)$, where $n = |\mathcal{I}|$. Equation (6) and Equation (7) ensure that the number of additional KV pairs is bounded by the chunk budget α . If the selected chunks introduce fewer than α additional KV pairs, we fill the chunk budget by selecting discrete KV pairs from the unselected positions in $\mathcal{W} \setminus \mathcal{U}$ according to score \mathbf{A}_i .

C.4 Pseudo Code and Implementation Details of the Periodic Compression Policy

The pseudocode of the periodic compression policy is presented in Algorithm 1. In our implementation with PagedAttention, the last block of a sequence is not always full. We therefore select sequences whose tail contains full and uncompressed blocks corresponding to \mathcal{W} tokens to form the compression window, and we exclude the last (possibly partial) block from compression. Since all selected sequences are compressed with the same window size, the blocks processed per sequence have the same shape. This allows us to process the selected sequences' windows in parallel during a compression event, including KV importance estimation, window-level memory compaction. To guarantee that we can always select sequences with $|\mathcal{W}|$ uncompressed tokens at the tail, we maintain a variable for each sequence that tracks the current number of uncompressed tokens at its end; this value is reset to 0 after each compression step.

D Additional Experiment Results

D.1 Additional Results for Figure 3(a)

We average the attention weights of each token's multi-head KV pairs and visualize the results across different layers in Figure 6. We consistently observe token x_i 's causal attention distribution largely matches its bidirectional attention distribution on preceding positions.

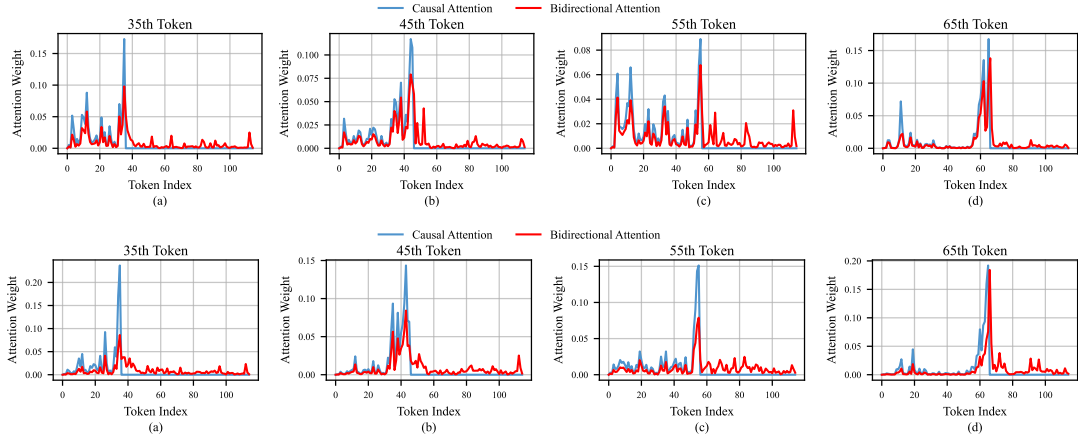


Figure 6: The top and bottom plots show the attention distributions of a token at Layer 10 and Layer 30, respectively.

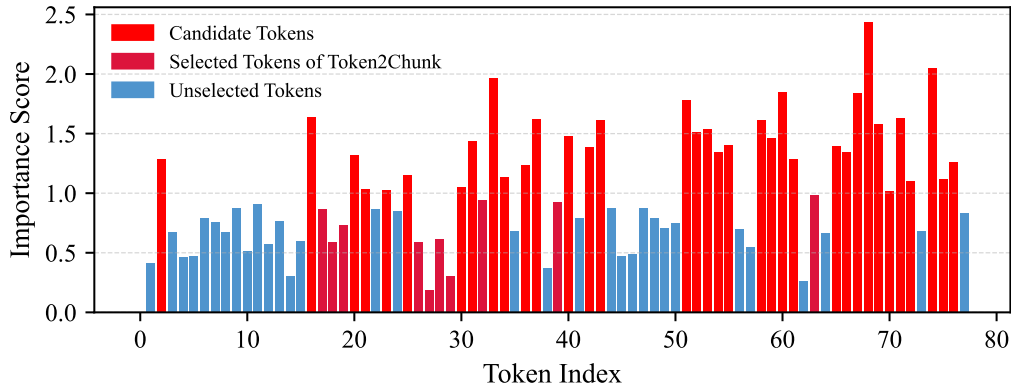


Figure 7: Visualization of the retained positions before and after applying Token2Chunk. We set the maximum chunk length and Token2Chunk budget to 7 and 10, respectively.

D.2 Visualization of Tokens Retained by Token2Chunk

We analyze several sequences sampled from MATH-500 and report one representative example. We visualize the importance scores of the first 80 tokens and indicate which positions are additionally selected by Token2Chunk. In this example, bidirectional attention scoring selects 35 discrete tokens, and we set the maximum chunk length and Token2Chunk budget to 7 and 10, respectively. We show the results for one representative layer and head. As shown in Figure 7, Token2Chunk helps recover contiguous semantic information that may be missed by discrete KV-pair selection alone.

D.3 Additional discussion of the results in Figure 5

We observe that RKV can be close to, or occasionally better than Kara in a few settings. We attribute this behavior to a difference in the effective *uncompressed inference length* before compression is activated. Concretely, for a given prompt, Kara starts compression once the number of uncompressed tokens reaches $|\mathcal{W}|$, whereas RKV typically starts compression only when the uncompressed cache length reaches a predefined threshold. In common configurations, this threshold is substantially larger than $|\mathcal{W}|$ (e.g., 2048 vs 384), which results in a longer uncompressed decoding trajectory for RKV. As a result, RKV may exhibit performance comparable to Kara in some cases.

However, RKV still relies on a threshold-triggered policy, which can incur frequent compression events under memory-constrained concurrent serving and degrade throughput. In contrast, Kara can

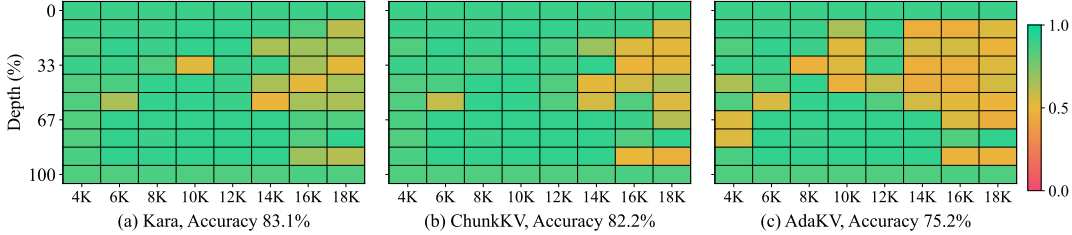


Figure 8: Needle-In-A-Haystack (NIAH) performance. The x-axis denotes the input context length and the y-axis denotes the needle insertion depth. Each cell reports the retrieval score for the corresponding (length, depth) setting, and we also report the mean accuracy averaged over all cells.

be integrated into KvLLM with a periodic compression schedule. In this setting, we can increase $|\mathcal{W}|$ to extend the uncompressed trajectory while controlling when compression is triggered, improving the throughput-quality trade-off under concurrency.

D.4 Results for NIAH Evaluation

In this experiment, a short needle statement is inserted into a long context at varying depths, and the model is queried to retrieve the needle. We follow standard NIAH setup [40] with context lengths up to 18,000 and report accuracy averaged over 10 depths. Figure 8 compares Kara with ChunkKV and AdaKV across different context lengths and insertion depths.

D.5 Latency and Throughput of KvLLM Framework

We report throughput and overall latency under different batch sizes for KvLLM, vLLM+SnapKV, and vanilla vLLM in Table 3. Note that when batch size is 16, 32, and 64, all frameworks are not memory-constrained, and all frameworks can maintain the maximum concurrency throughout decoding. As shown in Table 3, we observe that 1) at batch size 16, vLLM+SnapKV achieves the best throughput. This is because compression is not triggered frequently under small batch size, and compression reduces KV cache memory usage and thus reduces memory access latency, leading to higher throughput. In contrast, KvLLM shows no clear improvement over vanilla vLLM in this setting, as KvLLM introduces additional recomputation overhead and the resource constraint is not binding. 2) At batch sizes 32 and 64, neither vLLM+SnapKV nor KvLLM provides throughput gains. One possible reason is that the increased batch size raises the compression overhead itself (e.g., query cache storage in SnapKV and recomputation in KvLLM), offsetting potential benefits. 3) At batch sizes 128 and 256, KvLLM yields clear throughput improvements. In these memory-constrained settings, the available KV cache memory decreases rapidly during decoding, causing many sequences to wait and reducing realized concurrency. KvLLM releases PagedAttention blocks through periodic compression, allowing more sequences to participate in decoding and improving throughput. We can also tune the compression period to ensure that the compression overhead is covered by the resulting gains.

We also record the number of active running sequences across different decoding steps at batch size 256 in Figure 9. KvLLM maintains substantially higher active concurrency than vanilla vLLM at batch size 256, which is consistent with the observed throughput improvements.

Table 3: The overall latency (Lat.) in seconds and average throughput (Thr.) of different frameworks under various batch sizes (i.e., predefined maximum running sequences).

Batch Size	16		32		64		128		256	
	Lat. (s)	Thr. (tokens/s)	Lat. (s)	Thr. (tokens/s)	Lat. (s)	Thr. (tokens/s)	Lat. (s)	Thr. (tokens/s)	Lat. (s)	Thr. (tokens/s)
vLLM	2,263	390	1,558	707	1,155	1,457	884	2,633	678	2,943
vLLM + SnapKV	2,255	403	1,562	704	1,171	1,377	920	2,341	738	2,556
KvLLM	2,260	393	1,569	701	1,163	1,421	864	2,912	640	3,392

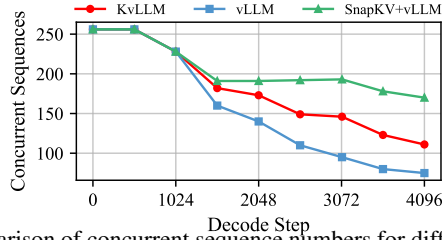


Figure 9: Comparison of concurrent sequence numbers for different frameworks.

D.6 Complexity Analysis of Kara

We analyze the computation complexity of applying Kara once to a single sequence, ignoring memory access and KV movement. Let the current sequence length be S , the sliding-window length be $W = |\mathcal{W}|$, and the protected buffer length be $U = |\mathcal{U}|$. Thus, the computational complexity of Kara can be formulated as:

$$T_{\text{Kara}} = O(LWSD + LWD^2 + LW(W - U)D + LH(W - U)), \quad (12)$$

where the first term denotes the attention cost of the additional recomputation forward pass over the current window, the second term denotes the query projection and FFN cost in the recomputation, the third term denotes the cost of sliding-window bidirectional attention for KV importance estimation, and the fourth term denotes the complexity of Token2Chunk.

SnapKV has a computation complexity of

$$T_{\text{SnapKV}} = O(LU(S - U)D), \quad (13)$$

where U denotes the query-buffer length.